Eur. Phys. J. A **13**, 169–175 (2002)

THE EUROPEAN PHYSICAL JOURNAL A

Giant-resonance studies with radioactive beams: Perspectives

M.N. Harakeh

Kernfysisch Versneller Instituut, Zernikelaan 25, 9747 AA Groningen, The Netherlands

Received: 1 May 2001

Abstract. First-generation radioactive ion-beam facilities have already been in operation for some time. Advanced facilities that will deliver high-intensity radioactive nuclear beams ranging in energy from below the Coulomb barrier to up to several hundred MeV per nucleon (MeV/u) are either starting operation, or under construction or in the planning stage. In this paper the perspectives of using radioactive nuclear beams to study giant resonances in nuclei far from the valley of stability are explored. In particular, emphasis will be made on information on certain nuclear properties that can be gained from such studies.

PACS. 21.65.+f Nuclear matter – 24.30.Cz Giant resonances – 24.50.+g Direct reactions

1 Introduction

With the advent of facilities that provide radioactive nuclear beams, the nuclear-physics research has moved towards new frontiers where new phenomena are expected to emerge from the study of nuclei far from the valley of stability. The study of giant resonances (GRs) in unstable nuclei becomes thus also possible and may strongly contribute to these developments. In fact, the study of GRs in stable nuclei has been one of the major fields of research in low-energy nuclear physics since the first systematic study of the isovector giant dipole resonance (IVGDR) in 1947 [1,2]; the first evidence for a giant-resonance excitation was found ten years earlier [3]. Since then this has proven to be a quite fruitful field of research, which not only taught us about the structure of these fundamental modes of excitation of the nucleus but also about some fundamental bulk properties of nuclei and nuclear matter [4].

The experimental study of GRs in unstable nuclei presents a real challenge. Whereas it has been possible to investigate GRs in stable nuclei by bombarding targets of the nuclei of interest by various probes, chosen depending on the spin and isospin structure of the multipole to be investigated, this will not be possible with unstable nuclei close to the proton or neutron drip line. It will be practically impossible to make targets of sufficient density to be useful for such studies. On the other hand, experiments can be performed in inverse kinematics, where beams of unstable nuclei impinge on a fixed target. This technique is now being developed for radioactive ion beams [5] but has been used with stable beams already in order to investigate the double-phonon excitation in nuclei [6]. This will be discussed in more detail below. Another possibility is to use collider rings where one of the rings is used for accelerating and storing the unstable nuclei and the other for accelerating and storing the beams that will be used as probes for giant-resonance excitation. Plans to build such collider rings with electron beams exist at RIKEN and GSI. Considering that various probes need to be used to disentangle the various multipole strengths and their spin and isospin structure, it is very strongly recommended to have the option of accelerating and storing in one of the collider rings proton, deuteron, ^{3}He, and α beams in addition to the electron beam. Especially for the study of the compression modes, the isoscalar giant monopole resonance (ISGMR) and isoscalar giant dipole resonance (ISGDR), the use of an α beam is imperative [4].

Now that high-intensity radioactive nuclear beams will soon be available at energies where excitation of giant resonances of various multipolarities and spin and isospin structure becomes possible, the following question arises. What new things can we hope to learn from the study of giant resonances in nuclei far from the stability valley, and in particular for the nuclei that are on the neutron-rich side of this valley? Although this question may lead to a wide variety of possible interesting answers regarding various aspects of nuclear structure and properties, I will address here only a few topics on which, I believe, information can be gained in the first stages of research on giant resonances in unstable neutron-rich nuclei. These are:

– The study of the ISGMR in a long chain of isotopes [7–9] in order to pin down the dependence of the nuclear incompressibility on the nuclear asymmetry, $(N-Z)/A$. This is important to fix the isospin dependence of the effective residual nucleon-nucleon interaction, *e.g.* by reproducing the ISGMR energies in the doubly closed-shell nuclei ^{100}Sn, ^{132}Sn and ^{208}Pb, as well as allow a more precise determination of the incompressibility of nuclear matter. Also, the equation of state of asymmetric matter may be better determined.

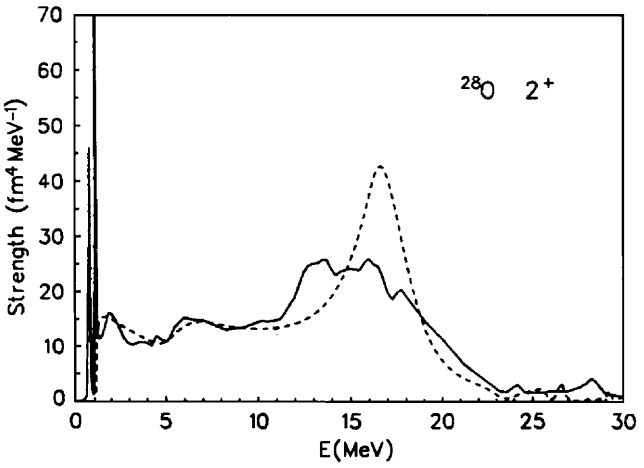

Fig. 1. The results of continuum RPA calculations obtained from ref. [12] without (dashed curve) and with (solid curve) coupling to surface vibrations.

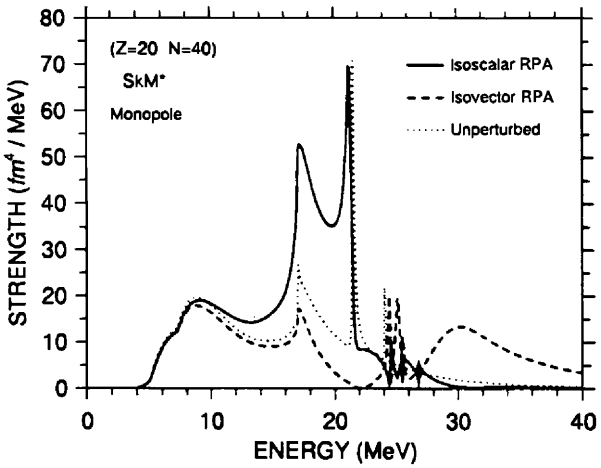

Fig. 2. RPA calculations with SkM* interaction for monopole strength in ^{60}Ca obtained from ref. [20].

– Determination of Gamow-Teller (GT) strength in unstable neutron-rich *sd*- and *fp*-shell nuclei. This has implications on supernova explosions and on the formation of neutron stars.
– Use of giant resonances as tools to determine neutron-skin thickness such as in the nuclear excitation of the IVGDR by isoscalar probes, or by the excitation of the isovector spin-flip dipole resonance (IVSGDR) in charge-exchange reactions [10,11].

2 Multipole strength functions in unstable nuclei

There has been a flurry of theoretical activity in the last decade aiming at investigating the structure of unstable nuclei. This was an anticipation of the near-future availability of the radioactive nuclear beams and the wide field of research that would open up. The giant-resonance structure in unstable nuclei, and in particular those with an extreme N/Z value, was studied. These calculations were performed for doubly closed-shell nuclei in order to avoid complications of pairing and deformation effects. The quadrupole (see, *e.g.*, refs. [12–18]) and dipole [19,17] response has been calculated for ^{28}O, and the monopole response for a number of calcium isotopes [20,21]. All these calculations have been performed in the self-consistent Hartree-Fock (HF) random-phase approximation (RPA) framework using a Skyrme-type interaction. The general feature that emerges from these calculations is the occurrence of low-lying non-collective strength. This is quite pronounced for neutron-rich drip line nuclei, but is also already evident for the less neutron-rich nuclei in the form of the known pygmy resonances.

The new features can be qualitatively understood from the unperturbed response functions of the neutron-rich nuclei. In these nuclei the proton well calculated in HF is much deeper than the neutron one due to the excess neutrons and the n-p interaction which is stronger than the n-n and n-p ones. The results for ^{28}O [22] indicate that the proton single-particle orbitals are more deeply bound than the neutron ones and that the shell gaps near the Fermi surface are larger for protons than for neutrons. Furthermore, since neutron orbitals just above the Fermi surface are slightly unbound, neutron excitations across the shells near the Fermi surface can lead to the threshold strength. This is observed, for example, in the calculations for the quadrupole response in ^{28}O [22,12]. In fig. 1, the results of the calculations by Ghielmetti *et al.* [12] are shown. The dashed curve corresponds to the results of the continuum RPA response for the isoscalar giant quadrupole resonance (ISGQR). The threshold strength displays strong sharp peaks, but low-lying non-collective strength appears in the whole excitation energy region below 10 MeV. The effect of coupling to surface vibrations (the first step in spreading) on the ISGQR is shown by the solid curve. The shape of the main peak is broader and the mean energy is lower. However, the non-collective low-lying strength is hardly affected.

A similar situation occurs for the monopole response in the Ca isotopes. The RPA monopole response has been calculated by Hamamoto *et al.* for ^{34,40,48,60}Ca [20,21] using the SkM* interaction. The monopole response for the neutron-rich drip line nucleus ^{60}Ca is shown in fig. 2. Although the main ISGMR strength is concentrated around 20 MeV, there is clearly low-lying non-collective strength due to neutron excitations in the region $E_x \approx 4$–12 MeV. Similar to the quadrupole case, the threshold strength develops for drip line nuclei.

The variation of the electric dipole response as a function of the neutron excess was calculated in large-scale shell-model basis by Sagawa and Suzuki [23]. The results of these calculations are interesting because for the lighter oxygen isotopes they can already be compared with experiment.

Experimentally there is nothing known about the multipole strength in unstable nuclei except for the recent experiments done at GSI to investigate the giant dipole resonance in neutron-rich oxygen isotopes. In these

experiments use is made of the technique of Coulomb excitation in inverse kinematics, a technique developed by the LAND collaboration at GSI to study multiphonon excitations. These experiments require a beam at an energy of several hundred MeV/u. On bombarding a heavy target, such as ^{208}Pb, the projectile nuclei are excited by absorbing virtual photons. This favours electric dipole excitation and the excitation cross-section is strongly dependent on the excitation energy. This is illustrated in fig. 3. In the upper frame, a smoothed reproduction of the measured ^{18}O(γ, n) cross-section is shown. In the lower frame, the expected differential cross-section for dipole strength excitation in ^{18}O is shown when a Pb target is bombarded with an ^{18}O beam of 250 MeV/u and 1 GeV/u. Clearly, the increase of the differential cross-section at the peak of the IVGDR for the higher beam energy is drastic. Therefore, to overcome the suppression due to the adiabatic cut-off of the virtual photon spectrum and thus excite the IVGDR with cross-sections comparable to those in photoabsorption, a bombarding energy of several GeV/u is required.

In this type of experiments the decay products of the excited projectile are measured. From the deduced four momenta of all particles emitted after the inelastic scattering, the excitation energy of projectile and target are reconstructed. Furthermore, since the virtual photon spectrum can be accurately calculated the isovector dipole strength distribution can be unfolded from the measured differential cross-section. However, in comparing to experiments it is customary to fold the theoretical response function with the calculated virtual photon spectrum. The data obtained by Aumann *et al.* for the excitation of dipole strength in ^{20}O and ^{22}O at 585 and 516 MeV/u bombarding energy, respectively, compare rather well with the results of Sagawa and Suzuki [23] after folding with the virtual photon spectra.

For the study of other GRs such as the ISGQR, ISGMR and charge-exchange modes (see also sect. 3) reactions in inverse kinematics with targets of ^{1}H, ^{2}H, ^{3}H, ^{3}He and ^{4}He targets are needed. The option of collider rings, as discussed above, could indeed be very useful if one is interested in high resolution both in energy and scattering angle. The high resolution in energy will certainly be required if the microscopic structure of GRs is studied via particle decay to final states in residual nuclei.

3 Applications of GRs in unstable nuclei

3.1 ISGMR and nuclear incompressibility

The incompressibility of nuclear matter, $K_{\rm nm}$, is a basic quantity that gives a measure for the stiffness of nuclear matter against variations in density. This quantity cannot be measured directly, but for low nuclear temperatures it can be determined from the strength distributions of compression modes, in particular that of the ISGMR. One first determines for a given nucleus A the nuclear incompressibility K_A from the measured isoscalar monopole strength distribution. If all the monopole strength is concentrated

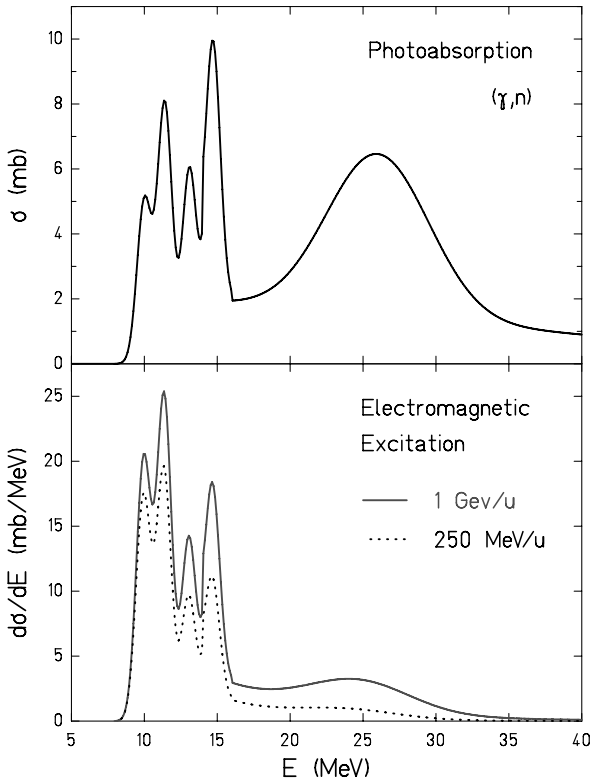

Fig. 3. Upper frame: The smoothed photo-absorption cross-section of ^{18}O [24]. Lower frame: Coulomb excitation cross-section for ^{18}O bombarding a ^{208}Pb target at 250 MeV/u (dotted curve) and 1 GeV/u (solid curve). From ref. [5].

in one single peak at energy E_0, K_A can be determined from the relation

$$E_0 = \sqrt{\frac{\hbar^2 K_A}{m\langle r^2\rangle}}\,, \tag{1}$$

where m is the nucleon mass and $\langle r^2\rangle$ the mean-square nuclear radius. $K_{\rm nm}$ is then determined from the experimental value of K_A on basis of a theoretical concept. Note that if K_A would be independent of A, $E_0 \propto A^{-1/3}$, which is what is found experimentally in $A \geq 90$ nuclei [4].

There are two models that are used to describe the ISGMR in finite nuclei: the constrained model and the scaling model. In the constrained model the nuclear incompressibility $K_A^{\rm C}$ is defined as

$$K_A^{\rm C} = \left[R^2 \frac{{\rm d}^2(E/A)}{{\rm d}R^2}\right]_{R=R_0}\,,$$

with the constraint $R_0^2 = \langle r^2\rangle_m$, the mean-squared mass radius. (E/A) is the HF binding energy of the nucleus A calculated as a function of $\langle r^2\rangle_m$. It can further be shown that [25,26]

$$\frac{\hbar^2 K_A^{\rm C}}{m\langle r^2\rangle_m} = (E_{\rm ISGMR}^{\rm C})^2 = \frac{m_1}{m_{-1}}\,, \tag{2}$$

where m_k is the moment of the monopole strength weighted by the k-th power of energy

$$m_k = \int \mathrm{d}\omega\ \omega^k S_{\mathrm{ISGMR}}\,,$$

and S_{ISGMR} is the monopole strength function derived from experiment.

In the scaling model, the vibrational motion is described as a scaling of the radial co-ordinates, $r(t) = r_0(1 + \alpha\cos\omega t)$. In this case the nuclear incompressibility K_A^{S} is given by [27]

$$\frac{\hbar^2 K_A^{\mathrm{S}}}{m\langle r^2\rangle_m} = (E_{\mathrm{ISGMR}}^{\mathrm{S}})^2 = \frac{m_3}{m_1}\,. \tag{3}$$

To derive the nuclear-matter incompressibility K_{nm} from the nuclear incompressibility K_A one can follow either a macroscopic or a microscopic approach. We will discuss here the macroscopic approach to illustrate the need for the measurement of the monopole strength in neutron-rich nuclei.

In the macroscopic approach K_A is derived from the second derivative of (E/A), the binding energy per nucleon of the semi-empirical mass formula, with respect to the radius. This will yield an expression for K_A as a sum of volume, surface, symmetry and Coulomb terms in analogy with the semi-empirical mass formula [27]

$$K_A = K_{\mathrm{V}} + K_{\mathrm{surf}}A^{-1/3} + K_{\mathrm{sym}}\left(\frac{N-Z}{A}\right)^2 + K_{\mathrm{Coul}}\frac{Z^2}{A^{4/3}} + \ldots \tag{4}$$

The interpretation of the various terms of this equation is complicated [25]. For example, The relation between K_{V} and K_{nm} is not straightforward but is model dependent: $K_{\mathrm{V}} = K_{(A\to\infty)} = \alpha K_{\mathrm{nm}}$. In the scaling model $\alpha = 1$, while in the constrained model $\alpha = 0.7$ [26]. Furthermore, in order to determine K_{V} accurately, the ISGMR should be measured in a wide range of nuclei. Because of the limited A range for which the ISGMR has been measured the separation of the various K_i terms becomes difficult since there exists a correlation between the various K_i terms. Although, the contribution of the symmetry term to K_A is small compared to that of the surface term, nevertheless it has an uncertainty similar to that of K_{V}. To remove the ambiguity due to the correlation between K_{V} and K_{sym}, the measurement of the ISGMR strength in a long chain of isotopes, *e.g.* the Sn isotopes, could help. Furthermore, this will help fix the isospin dependence of the effective nucleon-nucleon interaction.

To measure ISGMR strength in stable nuclei, the inelastic α-scattering at about 40–60 MeV/u and very forward scattering angles has been the tool of choice. The measurement of the ISGMR in, for example, unstable Sn isotopes would require measurements in inverse kinematics again at an energy of $\sim$ 40–60 MeV/u and very forward angles near and including 0°. To increase the luminosity, a ^{4}He gas target could be used in a ring for circulating unstable isotopes. However, as mentioned above colliding beams of α-particles and radioactive isotopes could be used if a collider, as discussed above, is realised.

3.2 GT strength in neutron-rich sd- and fp-shell nuclei

The accepted scenario for supernova type-II explosions is that massive stars having masses larger than ten times the solar mass, live for about 10^7 years (see ref. [28] and references therein). During this time the various burning cycles take place until a core of Fe-Ni, the nuclei with the highest binding energy per nucleon, is formed. As no further burning takes place to keep the pressure, gravitational collapse ensues. In this stage electron capture plays an important role, leading to the neutronisation of the core. At the beginning of the collapse, electron capture on free protons is important. However, at later stages where the energy of the electrons is such that the main GT strength can be reached, capture on nuclei becomes important [29]. Electron capture occurs on nuclei distributed around Fe-Ni in the upper *sd*- and lower *fp*-shell region. Therefore, it is important to know the GT matrix elements of the transitions that play a role in this case. It should be noted that Fermi matrix elements are zero because the Fermi transitions are completely Pauli blocked. The Pauli blocking for the GT transitions is not complete in the initial stages of neutronisation. As nuclei become very neutron rich also the GT transitions become Pauli blocked and further neutronisation proceeds via electron capture on free protons [30]. Gravitational collapse continues leading to an implosion within $\tau \sim 1$ s, followed by a shock wave which blows the mantle of the supernova leaving a neutron star at the core. The neutrinos diffuse into outer space in a characteristic time of $\tau \sim 10$ s.

Measuring the GT transitions mediated by the operator $\sigma\tau_+$ (GT_+ transitions) requires the use of (n, p)-type reactions at intermediate energies of around 150 MeV/u or higher. The GT_+ matrix elements for the important transitions can in principle be determined by means of the (n, p) reaction. In fact, in some cases where targets could be made the (n, p) reaction was used to determine the GT matrix elements [31,30]. However, the resolution that can be obtained is of the order of 1 MeV, not good enough to resolve low-lying GT transitions. Furthermore, for unstable nuclei charge-exchange reactions in inverse kinematics with neutrons as targets, are not feasible. In addition to the (n, p) reaction itself, the (d, ^{2}He), (t, ^{3}He) and heavy-ion charge-exchange reactions can be used. The (d, ^{2}He) reaction has been used in the past, but since two protons from the ^{2}He need to be measured in the outgoing channel, it makes the reaction mechanism and experimental procedure complicated. Recently, a good resolution has been achieved of about 150 keV which is sufficient for resolving most of the low-lying fragmented strength [32]. The (t, ^{3}He) reaction has been used in the past with primary triton beams at low bombarding energies [33]. The feasibility of using the (t, ^{3}He) reaction using secondary triton beams at intermediate energies has been demonstrated recently [34,35]. At these intermediate energies one expects a proportionality between the 0° (t, ^{3}He) cross-sections

and the GT matrix elements, as has demonstrated to be the case for the (^{3}He, t) reaction at 150 MeV/u [36,37]. Because of the better resolution that could be achieved, the (t, ^{3}He) reaction is better suited than the (n, p) reaction for studying low-lying fragmented GT strength [35]. With the possibility to use primary triton beams at intermediate energies [38] an even better energy resolution can be expected making the (t, ^{3}He) reaction the most suitable reaction for measuring GT_+ transition strength.

These other reactions, *i.e.* the (d, ^{2}He), (t, ^{3}He) and heavy-ion charge-exchange reactions, allow the study of GT_+ strength in unstable nuclei with reactions in inverse kinematics. Moreover, because of the better energy resolution and the simpler reaction mechanism and experimental procedure, the (t, ^{3}He) reaction becomes the reaction of choice to study GT_+ strength in unstable neutron-rich nuclei. This reaction lends itself to an easy implementation in collider rings as well.

3.3 Neutron-skin thickness of neutron-rich nuclei

Determining the shape of the nuclear-matter distribution of nuclei has been a subject of interest from the beginning when it became clear that nuclei have finite sizes. The charge distribution could be nicely determined with elastic electron scattering [39]. Different methods have been used to determine the neutron distribution or neutron-skin thickness using hadronic probes (see refs. [40,11] and references therein). In two of these methods the excitation of GRs has been used to infer the neutron-skin thickness.

In one of these methods, use is made of the fact that the cross-section for excitation of the IVGDR by inelastic scattering of isoscalar probes is sensitive to the neutron-skin thickness, $\Delta R_{\rm np} = (R_{\rm n} - R_{\rm p})$. In inelastic scattering the amplitude of the IVGDR excitation has two contributions, one due to the Coulomb interaction and the other due to the hadronic interaction [41]. The amplitude due to the isoscalar hadronic interaction is proportional to $\Delta R_{\rm np}$. DWBA calculations for the ^{208}Pb(α,α') IVGDR cross-section for several values of the neutron-proton radii difference $\Delta R_{\rm np}$ show that the cross-sections are relatively small but rather sensitive to $\Delta R_{\rm np}$.

Krasznahorkay *et al.* [10,40] studied inelastic α-scattering from the spherical nuclei ^{116,124}Sn and ^{208}Pb, and the deformed nucleus ^{150}Nd. The challenge in these experiments is to measure in an inelastic (α,α') experiment an IVGDR excitation cross-section of a few mb sr^{-1} spread out over a few MeV. It is by far too small to observe it directly as an enhancement over the continuum in the inelastic-scattering spectrum. This is the more so since the IVGDR and the ISGMR have approximately the same centroid energy and the ISGMR excitation differential cross-section in (α,α') reaction is of the order of 100 mb sr^{-1}. The IVGDR excitation cross-section can only be determined through a measurement of the cross-section in coincidence with γ-decay which is a very selective tool for detecting the IVGDR. The disadvantage is that the γ-decay branch of the IVGDR is very small, of $\sim 1\%$, but is known accurately from photo-absorption experiments, which is necessary in order to derive the IVGDR cross-section.

In these experiments the IVGDR/ISGMR were excited by the (α,α') reaction at 120 MeV bombarding energy and in the angular interval $(0\pm3)^\circ$. The final-state spectra populated by γ-decay from the excitation energy region of the IVGDR, are reconstructed from the two-dimensional coincident $(\alpha,\alpha'\gamma)$ spectra. The cross-sections for the excitation of the IVGDR can be evaluated from the peak corresponding to the ground-state γ-decay. Finally, by comparing the measured and calculated cross-sections, the $\Delta R_{\rm np}$ value can be determined. The $\Delta R_{\rm np}$ values determined in this method are found to be in agreement with values determined by other methods and also in agreement with the theoretical values [40].

With this method also the ratio of deformation of neutrons to that of protons can be determined. The result for the deformed nucleus ^{150}Nd is

$$\beta_2^{\rm n}/\beta_2^{\rm p} = 0.92 \pm 0.08\,.$$

Note that the result obtained from pion charge-exchange reactions on polarised ^{165}Ho is [42]

$$\beta_2^{\rm n} = (0.84 \pm 0.08)\beta_2^{\rm p}\,.$$

The two experiments using very different techniques agree in that they both find a larger deformation for protons than for neutrons, which must be due to the repulsive Coulomb interaction.

This method is, in principle, also useful to determine the neutron-skin thickness of unstable radioactive nuclei if such nuclei are available as beams with an energy $\geq$ 40 MeV/u. In inverse kinematics, the beam of unstable particles bombards a $T = 0$ target such as ^{4}He or ^{12}C and the emitted γ-rays from the decay of the IVGDR excited in the beam particle would be measured in coincidence with the scattered beam particle. However, owing to the very small cross-sections and the luminosities lower than what can be obtained with stable beams, this seems to be an impractical method for radioactive beams.

Another promising method to measure the neutron-skin thickness of neutron-rich nuclei is suggested by the fact that the sum rule for the spin-flip and non-spin-flip charge-exchange dipole resonances depends on $(N\langle r^2\rangle_{\rm n} - Z\langle r^2\rangle_{\rm p})$ [4]. Krasznahorkay *et al.* [11] have showed this in an experiment where $\Delta R_{\rm np}$ values were obtained from an analysis of the excitation cross-sections of the $\Delta L = 1$ IVSGDR in Sn nuclei using the (^{3}He, t) charge-exchange reaction at 150 MeV/u.

The IVSGDR with $\Delta L = 1$ mediated by the operator $[rY_1\sigma\tau]$ has three components with $\Delta J^\pi = 0^-, 1^-, 2^-$. A non-energy-weighted sum rule (NEWSR) for the spin-dipole operator involving the β^- and β^+ strengths is [4]:

$$S_-(\text{IVSGDR}) - S_+(\text{IVSGDR}) = \frac{9}{2\pi}(N\langle r^2\rangle_{\rm n} - Z\langle r^2\rangle_{\rm p})\,. \tag{5}$$

Another expression involving $S_\pm$(IVSGDR) can be obtained from the expression for S^+/S^- which describes the

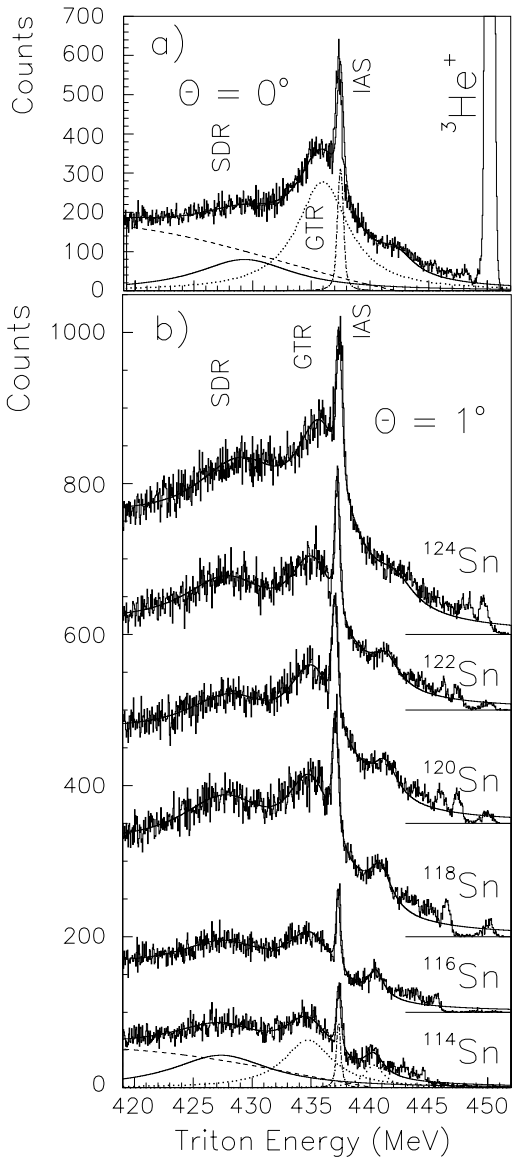

Fig. 4. (^{3}He, t) spectra on ^{114,116,118,120,122,124}Sn obtained at a beam energy of 150 MeV/u and at a scattering angle of a) 0° (only for ^{124}Sn) and b) 1° (all isotopes). The solid line is a fit taking into account the IAS, GTR and IVSGDR (label SDR in figure) and the continuum assumed to be due to quasi-free scattering. From ref. [11].

numerical results of the RPA calculations performed for the IVSGDR in the Sn isotopes [43,4]

$$S^+/S^- = 0.388 - 0.012(N-Z)\,,$$

which together with eq. (5) yield, after some algebra,

$$\Delta R_{\rm np} = (\langle r^2\rangle_{\rm n}^{1/2} - \langle r^2\rangle_{\rm p}^{1/2}) = \frac{[\,0.612 + 0.012(N-Z)]\alpha\sigma_{\rm exp} - (N-Z)\langle r^2\rangle_{\rm p}}{2N\langle r^2\rangle_{\rm p}^{1/2}}\,. \quad (6)$$

Here, $\sigma_{\rm exp}$ is the IVSGDR experimental cross-section, and α is a normalisation factor chosen such that for one isotope the experimental value for $\Delta R_{\rm np}$ equals the theoretical value.

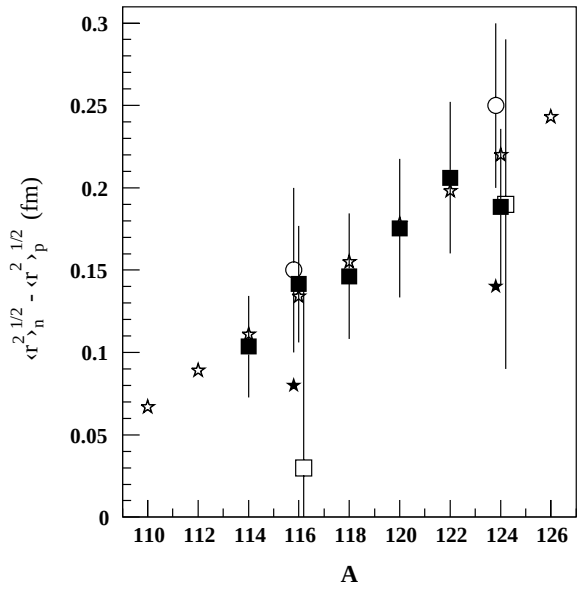

Fig. 5. $\Delta R_{\rm np} = (\langle r^2\rangle_n^{1/2} - \langle r^2\rangle_{\rm p}^{1/2})$ as a function of mass number for Sn isotopes. The calculated values are indicated by stars. The experimental values indicated by full squares are normalised to the calculated value for ^{120}Sn. Empty dots and squares are experimental values. The figure is from [11], where all symbols are explained.

In the experiment, (^{3}He, t) spectra for the isotopes ^{114,116,118,120,122,124}Sn were obtained at scattering angles of 0° and 1° using a beam energy of 150 MeV/u. Spectra are shown in fig. 4 [11]. The $\Delta L = 0$ excitations, the GTR and IAS, are relatively strongly excited at 0° and the IVSGDR at 1°. The spectra are deconvoluted into an IAS, GTR, IVSGDR for which a Breit-Wigner shape is assumed and a charge-exchange quasi-free continuum.

Using eq. (6), and adjusting the normalisation factor, α, for ^{120}Sn, the results shown in fig. 5 are obtained. There is a very nice agreement between these results and the data obtained with other methods as well as with theoretical calculations [11,4].

This method would become independent of the theoretical calculation to which the $\Delta R_{\rm np}$ value is normalised if a proportionality between cross-section and B(IVSGDR) were obtained similar to that for the Fermi and Gamow-Teller transitions. This could be realised if known strong first-forbidden β transitions are also excited in (p, n) or (^{3}He, t) reactions at energies $\geq$ 150 MeV/u.

The great advantage of this method over the one discussed before is that in this case the cross-sections involved are much larger, of the order 10 mb sr^{-1} compared to 10 μb sr^{-1}, mainly because in the latter case the experiment requires the measurement of the IVGDR γ-decay which has a probability of $\sim 10^{-2}$. Thus, statistical uncertainties can be much smaller. A disadvantage is that since no specific signature for IVSGDR excitation is used, the cross-sections have to be determined from a deconvolution of the whole triton spectrum with all the

uncertainties involved, especially with respect to the parameterisation of the underlying continuum. In principle, this method can also be used for radioactive nuclei by using the (p, n), or (^{3}He, t) reaction in inverse kinematics, provided that beams of radioactive nuclei with energies of about 150 MeV/u or higher are available. The (^{3}He, t) reaction has a clear advantage from the experimental point of view, especially if collider rings are used.

I would like to thank the organisers for the opportunity to talk at this symposium which has been organised in honour of Masayasu Ishihara. He is a colleague for whom I have much admiration and respect especially for his untiring efforts in promoting the physics with radioactive nuclear beams (RNB). He has been a strong proponent for building major RNB facilities. I also would like to acknowledge my many colleagues with whom I have collaborated and discussed about the physics of giant resonances over the years. In particular, I would like to mention Mamoru Fujiwara, Joachim Jänecke, Attila Krasznahorkay and Adriaan van der Woude.

References

1. G.C. Baldwin, G.S. Klaiber, Phys. Rev. **71**, 3 (1947).
2. G.C. Baldwin, G.S. Klaiber, Phys. Rev. **73**, 1156 (1948).
3. W. Bothe, W. Gentner, Z. Phys. **71**, 236 (1937).
4. M.N. Harakeh, A. van der Woude, *Giant resonances fundamental modes of excitation of the nucleus* (Oxford University Press, Oxford, 2001) and references therein.
5. T. Aumann *et al.*, Nucl. Phys. A **649**, 297c (1999).
6. T. Aumann, P.F. Bortignon, H. Emling, Annu. Rev. Nucl. Part. Sci. **48**, 351 (1998) and references therein.
7. M.M. Sharma *et al.*, Phys. Rev. C **38**, 2562 (1988).
8. D.H. Youngblood, H.L. Clark, Y.-W. Lui, Phys. Rev. Lett. **82**, 691 (1999).
9. D.H. Youngblood, H.L. Clark, Y.-W. Lui, Nucl. Phys. A **649**, 49c (1999).
10. A. Krasznahorkay *et al.*, Phys. Rev. Lett. **66**, 1287 (1991).
11. A. Krasznahorkay *et al.*, Phys. Rev. Lett. **82**, 3216 (1999).
12. F. Ghielmetti *et al.*, Phys. Rev. C **54**, (1996) R2143.
13. M. Yokoyama, T. Otsuka, N. Fukunishi, Nucl. Phys. A **599**, 367c (1996).
14. I. Hamamoto, H. Sagawa, X.Z. Zhang, Phys. Rev. C **55**, 2361 (1997).
15. I. Hamamoto, H. Sagawa, X.Z. Zhang, Nucl. Phys. A **626**, 669 (1997).
16. F. Catara *et al.*, Nucl. Phys. A **614**, 87 (1997).
17. A. Vitturi, J. Phys. G **24**, 1439 (1998).
18. H. Sagawa, I. Hamamoto, X.Z. Zhang, Nucl. Phys. A **649**, 319c (1999).
19. I. Hamamoto, H. Sagawa, X.Z. Zhang, Phys. Rev. C **57**, (1998) R1064.
20. I. Hamamoto, H. Sagawa, X.Z. Zhang, Phys. Rev. C **56**, 3121 (1997).
21. H. Sagawa, I. Hamamoto, X.Z. Zhang, J. Phys. G **24**, 1445 (1998).
22. I. Hamamoto, H. Sagawa, X.Z. Zhang, J. Phys. G **24**, 1417 (1998).
23. H. Sagawa, T. Suzuki, Phys. Rev. C **59**, 3116 (1999).
24. D.J. McLean *et al.*, Phys. Rev. C **44**, 1137 (1991).
25. J.P. Blaizot, Phys. Rep. **80**, 171 (1980).
26. J.P. Blaizot *et al.*, Nucl. Phys. A **591**, 435 (1995).
27. J. Treiner, H. Krivine, O. Bohigas, Nucl. Phys. A **371**, 253 (1981).
28. S.E. Woosley *et al.*, Nucl. Phys. A **621**, 445c (1997).
29. H.A. Bethe *et al.*, Nucl. Phys. A **324**, 487 (1979).
30. E. Caurier *et al.*, Nucl. Phys. A **653**, 439 (1999) and references therein.
31. M.C. Vetterli *et al.*, Phys. Rev. Lett. **59**, 439 (1987).
32. S. Rakers *et al.*, to be published in Phys. Rev. C (2002).
33. F. Ajzenberg-Selove *et al.*, Phys. Rev. C **31**, 777 (1985).
34. I. Daito *et al.*, Phys. Lett. B **418**, 27 (1998).
35. B.M. Sherrill *et al.*, Nucl. Instrum. Methods Phys. Res. A **432**, 299 (1999).
36. M. Fujiwara *et al.*, Nucl. Phys. A **599**, 223c (1996).
37. M. Fujiwara *et al.*, Phys. Rev. Lett. **85**, 4442 (2000).
38. S. Brandenburg, private communication (2001).
39. C.W. de Jager, H. de Vries, C. de Vries, At. Data Nucl. Data Tables **14**, 479 (1974).
40. A. Krasznahorkay *et al.*, Nucl. Phys. A **567**, 521 (1994).
41. G.R. Satchler, Nucl. Phys. A **472**, 215 (1987).
42. J.M. Knudson *et al.*, Phys. Rev. Lett. **66**, (1991) 1026.
43. V.A. Rodin, M.H. Urin, private communication (1999).